DOI: 10.3901/CJME.2011.**.***, available online at www.cjmenet.com; www.cjmenet.com.cn

Multi-axial Fatigue of 2024-T4 Aluminum Alloy

WANG Xiaogui[1], GAO Zengliang[1, *] QIU Baoxiang[1], WANG Limei[1], and JIANG Yanyao[2]

1 *College of Mechanical Engineering, Zhejiang University of Technology, Hangzhou 310032, China*
2 *Department of Mechanical Engineering, University of Nevada, Reno, NV 89557, USA*

Received January 21, 2010; revised November 24, 2010; accepted December, 2010; published electronically December, 2010

Abstract: Only the fatigue initiation is considered by the safe-life design approach, while fatigue crack propagation is paid more attention by the damage tolerance approach. The reasonable fatigue design method and durability assessment standard should give these two phases equivalent concerns. To develop a unified model of fatigue initiation and crack propagation, a great deal of baseline fatigue properties of a material should be obtained by fatigue experiments. However, there is lack of thorough and comprehensive experiment study on the fatigue properties of 2024-T4 aluminum alloy, which is widely used as load-bearing components in aircraft industry. In this paper, strain-controlled uniaxial, torsion, and combined axial-torsion fatigue experiments are conducted on 2024-T4 aluminum alloy in ambient air. Fully reversed uniaxial and pure torsion experiments employ solid cylindrical specimens. Fatigue experiments under the fully reversed shear loading with a static axial stress, proportional axial-torsion loading, and 90° out-of-phase axial-torsion nonproportional loading are conducted by using thin-walled tubular specimens. The experimental results show that the mean stress has a significant influence on the fatigue strength of the material. A tensile mean stress decreases the fatigue life dramatically, while a compressive mean stress increases the fatigue life. The strain-life fatigue results obtained from the fully reversed uniaxial fatigue experiments can be represented by one smooth curve of a three-parameter equation. However, two fitting curves are needed for characterizing the results of the fully reversed pure torsion fatigue tests because of the existence of an obvious kink. The baseline fatigue properties of 2024-T4 aluminum alloy obtained from the fatigue experiments have applications for the fatigue design and safe assessment of engineering components.

Key words: 2024-T4 aluminum alloy, fatigue life, loading path, multiaxial fatigue, SWT fatigue parameter.

1 Introduction*

2024-T4 aluminum alloy is widely used in the modern industry because of the high ratio of strength to mass density. Fatigue due to cyclic loading is the most common failure form in the load-bearing structural components made of 2024-T4 aluminum alloy. The process of fatigue failure generally consists of two stages: fatigue crack initiation and fatigue crack propagation. Only the fatigue crack initiation is considered by the "safe-life design approach" which is widely adopted in the structural fatigue design of aircraft industry. On the other hand, the "damage tolerance approach" for the safety assessment of the in-service components pays more attention to fatigue crack propagation[1]. However, because these two different stages are based upon the same fatigue damage mechanism, they should be given equivalent concerns in the fatigue design and durability assessment of load- bearing component[2]. Although theoretical models and numerical simulations are widely used, the experimental investigations are of great importance to obtain the baseline fatigue properties of a material and to validate the fatigue models.

Strain-life approaches are widely used in the fatigue design. For most steel and copper materials, the elastic stress-life data could be linearized on log-log scale and the plastic strain-life usually follows the Coffin-Manson relationship. The resulting single slope curve of the total strain amplitude versus the fatigue life can be expressed as[3]

$$\frac{\Delta\bar{\varepsilon}}{2}=\frac{\sigma_{\rm f}}{E}(N_{\rm f})^{b}+\varepsilon_{\rm f}(N_{\rm f})^{c}, \qquad (1)$$

where $\Delta\bar{\varepsilon}/2$ is the total strain amplitude, $\sigma_{\rm f}$ is the fatigue strength coefficient, $\varepsilon_{\rm f}$ is the fatigue ductility coefficient, E is the elasticity modulus, $N_{\rm f}$ is the fatigue life in terms of number of cycles to failure, b is the fatigue strength exponent, and c is the fatigue ductility exponent. The first term of the right hand side of Eq. (1) is for the elastic strain part, and the second term for the plastic strain part. Both of the relationships between the elastic strain part and fatigue life as well as the plastic strain part and fatigue life are linear in the log-log scale. ENDO, et al[4], found that the

* Corresponding author. E-mail: zlgao@zjut.edu.cn
This project is supported by National Natural Science Foundation of China (Grant No. 50975260), and Zhejiang Provincial Natural Science Foundation of China (Grant No. Z1091027)

linear relations as given in Eq. (1) cannot give adequate correlations of 2024-T4 and 7075-T6 aluminum alloys. SANDERS, et al[5], argued that the observed poor correlation was due to the fact that the Coffin-Manson relationship was just applicable down to a material dependent critical level of plastic strain. In other words, if the plastic strain part is lower, the Coffin-Manson relationship no longer obeys the single slope behavior. FATEMI, et al [3], used the stress amplitude versus fatigue life curves of 14 aluminum alloys to validate the bi-linear relationship and found that it provided a better correlation than the single slope linear model. ZHAO, et al[6], observed that there was a kink associated with the cracking behavior around a fatigue life of 3×10^5 cycles in the shear strain-life curve of 7075-T651 aluminum alloy under pure torsion. The experimental data divided by the kink can be properly described by two equations.

Engineering structural components often experience nonproportional loading, and the states of stress and strain of the fatigue failure positions are generally multiaxial. Based on the fatigue damage parameter for uniaxial loading proposed by SMITH, WATSON, and TOPPER(SWT)[7], SOCIE[8], and FATEMI, et al[9], extended the SWT parameter to multiaxial fatigue with a critical plane interpretation, i.e.,

$$\varPsi = \sigma_{\max}\frac{\Delta\hat{\varepsilon}}{2}, \tag{2}$$

where $\varPsi$ is the SWT fatigue damage parameter, $\sigma_{\max}$ is the maximum stress in a loading cycle, and $\Delta\hat{\varepsilon}/2$ is the cyclic normal strain amplitude. The critical plane is defined as the material plane with maximum normal strain amplitude. The extended SWT parameter predicts a cracking plane whose normal is parallel to the axial stress direction for tension-compression loading, and ±45° cracking planes for pure torsion loading. JIANG, et al[10–12], defined the critical plane as the material plane which experienced the maximum fatigue damage. ZHAO, et al[6], modified the SWT parameter to consider the general stress state and cracking behavior. The modified SWT parameter was found to give better predictions of the fatigue life and cracking behavior of 7075-T651 aluminum alloy under multiaxial loading conditions. The SWT parameter is found to be particularly suitable for aluminum alloys.

Despite comprehensive work, the fatigue cracking behavior of the aluminum alloys under multiaxial stress-strain states has not been well investigated. To obtain the fundamental data of 2024-T4 aluminum alloy, extensive fatigue experiments were conducted under uniaxial, torsion, and axial-torsion cyclic loadings in the current study. The SWT parameter was evaluated.

The remainder of this paper is organized as follows. Section 2 presents the experimental conditions and results of multiaxial fatigue testing of 2024-T4 aluminum alloy. Section 3 gives the correlation of a SWT parameter to the experimental fatigue lives. In section 4 some conclusions are made.

2 Multi-axial Fatigue Experiments

2.1 Material and specimens

In the fatigue testing program of the 2024-T4 aluminum alloy, three kinds of cylindrical specimens were used, as shown in Fig. 1. They are the uniaxial solid cylindrical specimens (Fig. 1(a)), solid cylindrical specimens for fully reversed pure torsion (Fig. 1(b)), and the tubular specimens for multi-axial fatigue (Fig. 1(c)). Symbol D denotes the outer diameter of the tubular specimens or the solid cylindrical specimens, and d is the inner diameter of the tubular specimens. Symbol F denotes the axial force and T is the torque. All the specimens were fabricated from a cylindrical bar with a diameter of 60 mm. The axis of each specimen is parallel to that of the cylindrical bar. Before fatigue tests, the surface of the gauge section in the specimen was polished carefully to eliminate the effects of the micro-defects and residual stress on the fatigue properties induced by the mechanical processing. No additional heat treatment was made before and after the fabrication of the testing specimens.

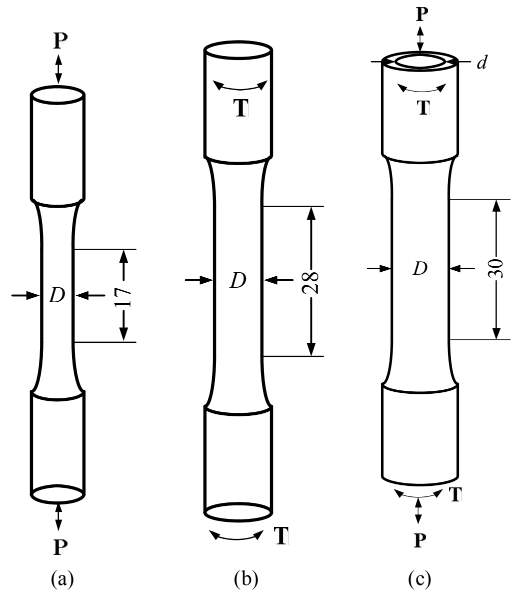

Fig. 1. Three kinds of cylindrical specimens

2.2 Experimental conditions

An Instron Servohydraulic tension-torsion load frame was used for the fatigue experiments. The testing system was equipped with the Instron 8800 electronic control, computer control, and data acquisition. The load cell of the testing system has a capacity of ±2 800 N • m in torque and ±222 kN in axial load. A uniaxial extensometer, whose gauge length is 12.7 mm and strain range is ±5%, was used for the measurement and control of the axial strain in the gauge section of the uniaxial specimens. For specimens used for the fully reversed torsion tests and multiaxial fatigue experiments, a modified MTS biaxial extensometer was used to measure the radial, circumferential, and axial strains. The biaxial extensometer has a range of $\pm 5\%$ in the axial strain, a range of $\pm 3°$ in the torsion deformation, and a 0.25 mm range in the radial direction. All the experiments were conducted in ambient air.

All the fatigue experiments were conducted under the strain-controlled condition. Fig. 2 shows the three loading paths used in the axial-torsion experiments for the tubular specimens. Where the horizontal axis denotes the $1/\sqrt{3}$ times of the shear strain γ, and the vertical axis represents the axial strain ε. Fig. 2(a) is the fully reversed shear loading with a static axial stress, Fig. 2(b) is the proportional axial-torsion loading, and Fig. 2(c) is the 90° out-of-phase axial-torsion nonproportional loading.

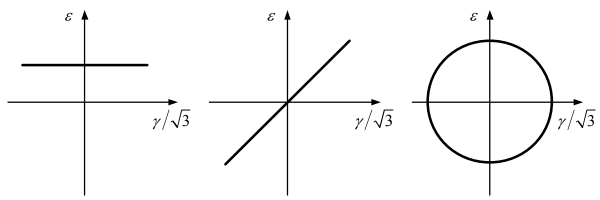

(a) (b) (c)

Fig. 2. Three loading paths used in the axial-torsion experiments for the tubular specimens

Detailed loading conditions and experimental fatigue lives are summarized in Tables 1–5. Where $\Delta\varepsilon/2$ is the controlled axial strain amplitude, $\Delta\sigma/2$ is the axial stress amplitude corresponding to $\Delta\varepsilon/2$, $\Delta\gamma/2$ is the controlled shear strain amplitude, and $\Delta\tau/2$ is surface shear stress amplitude corresponding to $\Delta\gamma/2$. σ_m is the applied static axial stress associated with the cyclic torsion loading for the tubular specimens. The loading frequency f was determined based on the rule that the influence of its change on the testing results should be insignificant. To this end, a lower loading frequency was selected for the higher loading amplitude, and a higher loading frequency was used for the lower loading amplitude. The loading frequency for each tubular specimen under combined axial-torsion loading was set to be lower than 2 Hz, which is not listed in Table 3–5.

The fatigue life, N_f, corresponds to the moment when the stress amplitude is reduced by 10% from the stabilized value, or when a visible crack is found on the surface of the gauge section. It is commonly believed that after about half of the fatigue life, the stress-strain response of the material of the gauge section will be stabilized. The stabilized hysteresis loops of axial stress versus axial strain are shown in Fig. 3. The reported axial stress amplitude $\Delta\sigma/2$ in Table 1 can be then easily obtained. The surface shear strain amplitude was a control parameter in the pure torsion experiments using the solid specimens. Following the procedure given by KALNAUS, et al[13], the corresponding surface shear stress amplitude $\Delta\tau/2$ can be determined by using the cyclic stress-strain curve obtained from testing the tubular specimens under fully reversed pure torsion loading. The shear stress amplitudes obtained through such procedure are listed in Table 3.

Table 1. Fatigue experiments under fully reversed uniaxial loading

Specimen No.	Loading frequency f/Hz	Outer diameter D/mm	Axial strain amplitude $\Delta\varepsilon/2$/ %	Axial stress amplitude $\Delta\sigma/2$/ MPa	Fatigue life N_f/cycle
ALUN04	0.125	11.32	2.00	618.4	12
ALUN08	1	11.24	1.50	576.7	35
ALUN01	0.25	11.19	1.00	554.1	127
ALUN19	1	11.56	0.80	526.4	184
ALUN05	0.5	11.18	0.70	522.2	660
ALUN18	1	10.38	0.60	456.4	1 780
ALUN07	2	11.31	0.50	387.4	5 400
ALUN11	1	11.26	0.40	311.1	15 921
UTN01	5	17.75	0.40	300.0	33 793
ALUN17	10	11.02	0.35	276.5	54 461
UTN03	5	17.66	0.35	264.0	123 244
ALUN14	10	11.12	0.30	234.7	146 061
ALUN13	10	10.82	0.30	229.1	196 703
UTN02	10	17.74	0.30	226.6	413 000
ALUN12	10	11.27	0.25	192.8	895 357

Table 2. Fatigue experiments under fully reversed pure torsion

Specimen No.	Loading frequency f/Hz	Outer diameter D/mm	Shear strain amplitude $\Delta\gamma/2$/ %	Surface shear stress amplitude $\Delta\tau/2$/MPa	Fatigue life N_f/cycle
UTN12	0.25	17.77	2.10	327.0	360
UTN04	0.2	17.63	1.61	320.0	800
UTN05	1	17.77	1.21	305.0	2 000
T01	1.5	17.46	0.97	266.0	3 300
UTN06	2	17.66	0.81	223.0	8 800
UTN11	2	17.55	0.73	201.0	17 400
UTN15	2	17.81	0.69	188.3	19 000
T02	1	17.00	0.64	176.0	27 618
UTN13	3	17.77	0.63	171.5	97 400
UTN08	3	17.81	0.65	180.1	141 348
UTN07	4	17.71	0.57	156.9	197 855
TN01	2	17.66	0.61	168.0	194 208
UTN10	5	17.61	0.54	148.1	260 000
TN02	2	17.66	0.50	140.2	489 033
UTN09	5	17.77	0.48	133.5	592 000
UTN14	5	17.65	0.48	134.8	973 616

Table 3. Fatigue experiments under fully reversed shear loading with a static axial stress

Specimen No.	Outer diameter D/mm	Inner diameter d/mm	Applied static axial stress σ_m/MPa	Shear strain amplitude $\Delta\gamma/2$/%	Surface shear stress amplitude $\Delta\tau/2$/MPa	Fatigue life N_f/cycle
TTF05	23.73	19.92	200.0	0.73	177.6	800
TTF03	23.59	19.99	0.0	0.73	193.7	2 300
TTF01	23.56	19.87	−100.0	0.73	193.3	142 150
TTF04	23.79	19.88	−200.0	0.73	196.5	16 600
TTF06	23.72	19.96	−100.0	0.69	186.8	118 400
TTF07	23.66	19.91	−200.0	0.69	184.4	68 400

Table 4. Fatigue experiments under proportional loading

Parameter	Specimen No.			
	NT03	NT02	TF08	NT01
Outer diameter D/mm	23.72	23.57	23.68	23.56
Inner diameter d/mm	19.91	19.86	19.90	19.88
Axial strain amplitude $\Delta\varepsilon/2$/ %	0.50	0.40	0.30	0.25
Shear strain amplitude $\Delta\gamma/2$/ %	0.85	0.68	0.51	0.43
Axial stress amplitude $\Delta\sigma/2$/ MPa	237.2	277.7	218.3	182.7
Surface shear stress amplitude $\Delta\tau/2$/MPa	136.9	169.7	133.8	114.1
Fatigue life N_f/cycle	910	4 400	16 600	74 800

Table 5. Fatigue experiments under 90° out-of-phase nonproportional loading

Parameter	Specimen No.			
	NT07	NT08	NT04	NT06
Outer diameter D/mm	23.79	23.80	23.69	23.45
Inner diameter d/mm	19.88	19.92	19.89	19.91
Axial strain amplitude $\Delta\varepsilon/2$/ %	0.50	0.35	0.30	0.25
Shear strain amplitude $\Delta\gamma/2$/ %	0.84	0.60	0.51	0.43
Axial stress amplitude $\Delta\sigma/2$/ MPa	360.8	255.4	213.6	187.4
Surface shear stress amplitude $\Delta\tau/2$/MPa	201.2	158.8	133.3	116.3
Fatigue life N_f/cycle	880	7 650	9 300	50 273

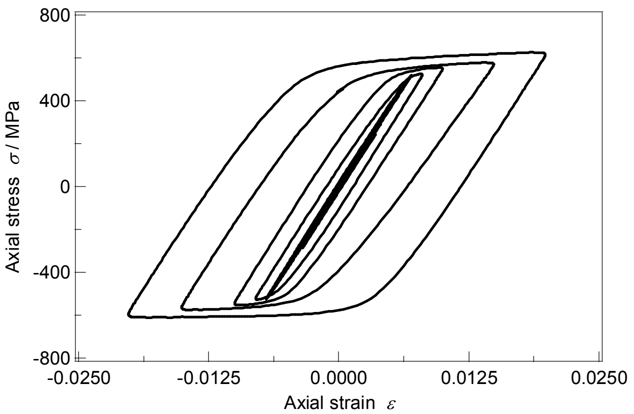

Fig. 3. Stabilized stress-strain hysteresis loops for fully reversed uniaxial tests

Before the fatigue experiment, several hundreds of fully reversed uniaxial loading cycles at very low level well below the yield stress were applied to each specimen. The axial stress is proportional to the axial strain in this kind of cyclic loading procedure. The linear elastic phase of the axial stress-strain curves was used to determine the elastic modulus E and the Poisson's ratio ν of 2024-T4 aluminum alloy. The least square technique was used to fit linearly the experimental data. The obtained elastic modulus is 73.1 GPa and Poisson's ratio is 0.33.

2.3 Experimental results

The detailed loading frequency, diameter of gauge section, axial stress amplitude, axial strain amplitude, and fatigue life for each fully reversed uniaxial experiment are listed in Table 1. The axial stress amplitude versus fatigue life is shown in Fig. 4, and the axial strain amplitude versus fatigue life is shown in Fig. 5. The following three-parameter equation was used to describe the strain-life curve

$$\left(\frac{\Delta\varepsilon}{2}-\varepsilon_0\right)^n N_f = C. \quad (3)$$

By best fitting the strain-life experimental data, the three material parameters, ε_0, n and C, can be determined. For 2024-T4 aluminum alloy, they are ε_0=0.002 6, n=2.8, and C=0.000 14. The curve of Eq. (3) with three fitted parameters is also given in Fig. 5. It is clear that the strain-life experimental data can be well described by using Eq. (3).

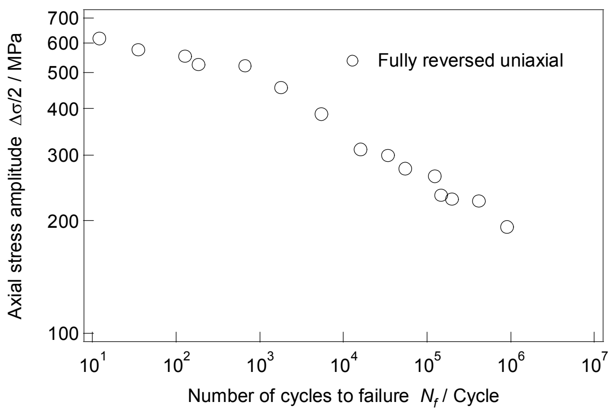

Fig. 4. Stress-life for fully reversed uniaxial loading

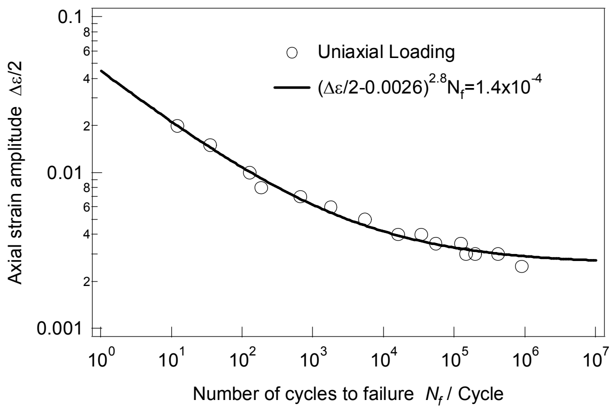

Fig. 5. Strain-life for fully reversed uniaxial loading

Fig. 6 shows the experimental strain-life obtained from the fully reversed pure torsion loading of solid cylindrical specimens. The detailed geometrical dimensions, loading conditions and fatigue life for each specimens are listed in Table 2. It can be found that there is a kink around a fatigue life of 2×10^5 cycles in the shear strain-life curve of the fully reversed pure torsion loading. Unlike the axial strain-life (Fig. 5) which can be properly described by Eq. (3), two three-parameter equations are needed to better describe the experimental data of the surface shear strain amplitude versus the fatigue life of the solid rod specimens. For

2024-T4 aluminum alloy, the fitted parameters are ε_0=0.005 4, n=1.85, and C=0.17, for fatigue life lower than 200 000 cycles; ε_0=0.004 7, n=0.7, and C=1 532 for fatigue life longer than 200 000 cycles.

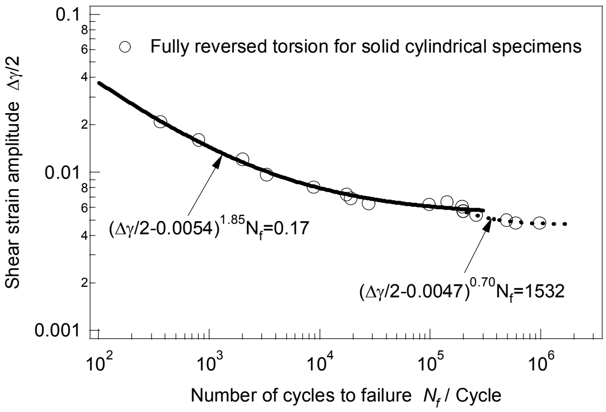

Fig. 6. Strain-life for fully reversed pure torsion loading

To study the effects of the mean stress on the fatigue property of 2024-T4 aluminum alloy, two shear strain amplitudes with different static axial stresses were used for a loading path shown in Fig. 2(a). The detailed loading conditions are given in Table 3. Fig. 7 shows the experimental results. It is clear that with shear strain amplitude of 0.73%, a positive static axial stress reduces the fatigue life, while a compressive static axial stress enhances the fatigue life. Moreover, for both tested shear strain amplitudes, a smaller axial compression load leads to a longer fatigue life. The mean stress was found to have a significant influence on the fatigue strength of the material.

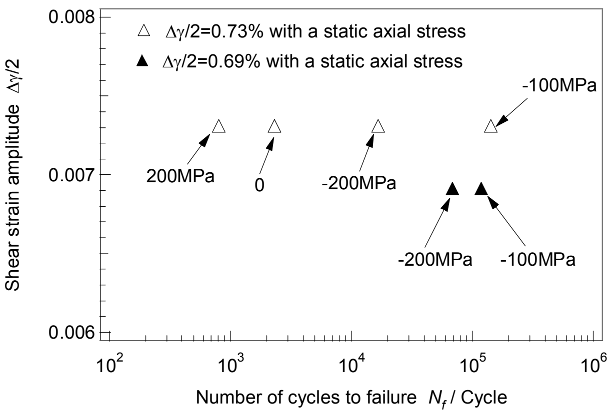

Fig. 7. Strain-life for fully reversed shearing loading with a static axial stress

The experimental results of the tubular specimens under combined axial-torsion loading are shown in Fig. 8. The detailed loading conditions and results are listed in Tables 4–5. An equivalent strain amplitude, $\Delta\varepsilon_{eq}/2$, defined as follows:

$$\frac{\Delta\varepsilon_{eq}}{2}=\sqrt{\left(\frac{\Delta\varepsilon}{2}\right)^2+\frac{1}{3}\left(\frac{\Delta\gamma}{2}\right)^2}, \quad (4)$$

was used to represent the combined axial-torsion cyclic loading magnitude. It is clear that, for the same equivalent strain amplitude, the fatigue life with respect to the loading path (b) is longer than that with respect to the loading path (c) when the fatigue life is longer than 10^4 cycles. The loading path has a significant influence on the fatigue life of 2024-T4 aluminum alloy in the case of high cycle fatigue.

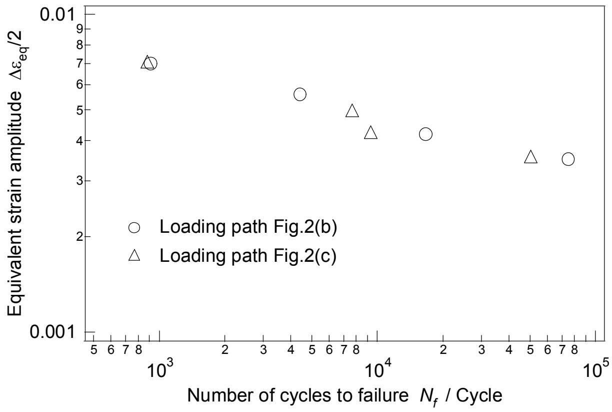

Fig. 8. Fatigue under combined axial-torsion loading

3 SWT Fatigue Parameter Correlation with Experiments

The SWT fatigue parameter with the critical plane concept as given in Eq. (2) has been commonly recognized to be particularly suitable for aluminum alloys. The normal strain amplitude and the maximum normal stress in the expression of SWT parameter are taken on the critical plane. For the fully reversed uniaxial loading, the critical plane is identical to the cross section of the cylindrical specimens. Because the uniaxial loading is fully reversed, $\Delta\varepsilon/2$ is taken to be the controlled axial strain amplitude and σ_{max} is equal to the axial stress amplitude. For the fully reversed pure torsion loading, the critical plane takes an angle of 45° with the axis of the cylindrical specimens. Since the pure torsion loading is also fully reversed, σ_{max} and $\Delta\varepsilon/2$ are equal to the surface shear stress amplitude and half of the controlled shear strain amplitude, respectively, i.e., $\sigma_{max}=\Delta\tau$ and $\Delta\varepsilon/2=\Delta\gamma/4$. However, in the case of cyclic axial-torsion loading paths, the coordinate transformation of stress and strain components should be used to determine the critical plane and the stress strain components on the critical plane.

The value of SWT parameter for the fully reversed uniaxial loading is equal to the product of the controlled axial strain amplitude (the forth column of Table 1) and the axial stress amplitude (the fifth column of Table 1). For the fully reversed pure torsion loading, the SWT parameter is equal to half the product of the controlled shear strain amplitude (the forth column of Table 2) and the surface shear stress amplitude (the fifth column of Table 2). The calculated SWT parameter versus the experimental fatigue life for solid cylindrical specimens under fully reversed uniaxial and pure torsion loadings are shown in Fig. 9.

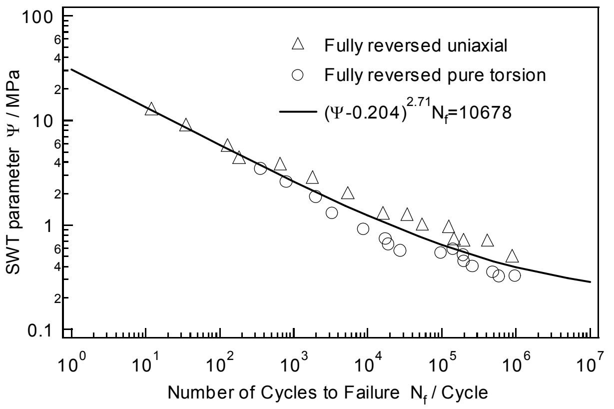

Fig. 9. SWT parameter versus the experimental fatigue life for solid cylindrical specimens under fully reversed uniaxial and pure torsion loadings

The following three-parameter equation identical to Eq. (3) mathematically

$$(\Psi - \Psi_0)^n N_f = C \quad (5)$$

was used to characterize the relationship between the SWT parameter and the fatigue life. By better fitting the experimental data, the three material parameters were determined to be Ψ_0=0.204, n=2.71, and C=10 678. It is clear that the fitted three-parameter equation correlates the experimental fatigue life well.

For each specimen, the SWT parameter, Ψ, can be determined. By using Eq. (5), the fatigue life of the specimen can be predicted. A comparison between the predicted fatigue lives and the observed lives for all the specimens tested in the current investigation is shown in Fig. 10.

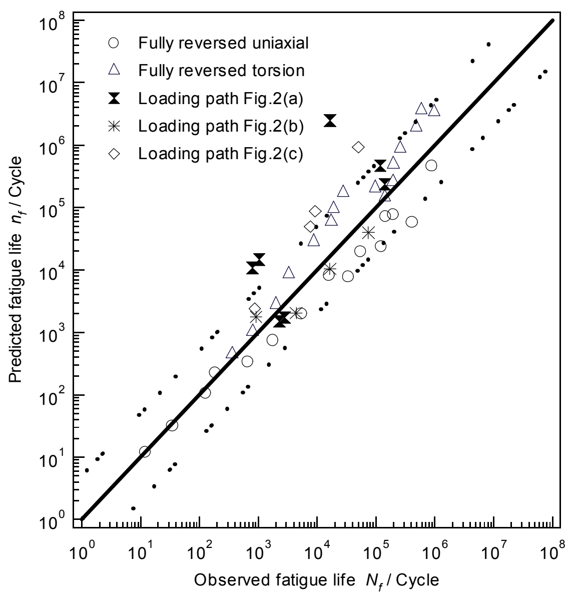

Fig. 10. Comparison between the predicted fatigue lives and the observed lives for all the specimens tested in the current investigation

The solid diagonal line in Fig. 10 denotes a perfect prediction and the two dotted lines are the factor-of-five boundaries. It is obvious that Eq. (5) can correlate well most of fatigue experiments. However, the predicted results are very poor for the fatigue experiments under fully reversed shear loading with a static compressive axial stress of −200 MPa.

4 Conclusions

(1) An axial mean stress has a significant effect on the fatigue strength of material subjected to cyclic torsion loading. A positive mean stress reduces the fatigue life, while the compressive mean stress enhances the fatigue life. However, a larger (absolute) axial compressive stress results in shorter fatigue life as compared with that under a smaller axial compressive stress.

(2) The experimental data of axial strain versus fatigue life under fully reversed uniaxial loading can be well described by one three-parameter strain-life equation, while two such equations are needed for the case under fully reversed pure torsion.

References

[1] HOFFMAN M E, HOFFMAN P C. Current and future fatigue life prediction methods for aircraft structures[J]. *Naval Research Reviews*, 1998, 50(4): 55–68.
[2] JIANG Y, FENG M L. Modeling of fatigue crack propagation[J]. *ASME Journal of Engineering Material and Technology*, 2004, 126(1): 77–86.
[3] FATEMI A, PLASEIED A, KHOSROVANEB A K, et al. Application of bi-linear log-log S-N model to strain-controlled fatigue data of aluminum alloys and its effect on life predictions[J]. *International Journal of Fatigue*, 2005, 27(9): 1 040–1 050.
[4] ENDO T, MORROW J. Cyclic stress-strain and fatigue behavior of representative aircraft metals[J]. *Journal of Materials*, 1969, 4(1): 159–175.
[5] SANDERS T H, MAUNEY D A, STALEY J T. Strain control fatigue as a tool to interpret fatigue initiation of aluminum alloys[M]//JAFFEE R I, WILCOX B A, eds. *Fundamental aspects of structural alloy design*, New York: Plenum Publishing, 1977.
[6] ZHAO T, JIANG Y. Fatigue of 7075-T651 aluminum alloy[J]. *International Journal of Fatigue*, 2008, 30(5): 834-849.
[7] SMITH R N, WATSON P, TOPPER T H. A stress-strain parameter for the fatigue of metals[J]. *Journal of Materials*, 1970, 5(4): 767–778.
[8] SOCIE D F. Multiaxial fatigue damage models[J]. ASME *Journal of Engineering Material and Technology*, 1987, 109(4): 293–298.
[9] FATEMI A, SOCIE D F. A critical plane approach to multiaxial fatigue damage including out of phase loading[J]. *Fatigue & Fracture of Engineering Material & Structure*, 1988, 11(3): 149–165.
[10] JIANG Y, SEHITOGLU H. *Fatigue and stress analysis of rolling contact*[R]. Report No. 161, UILU-ENG 92-3602, University of Illinois at Urbana-Champaign, 1992.
[11] JIANG Y. A fatigue criterion for general multiaxial loading[J]. *Fatigue & Fracture of Engineering Material & Structure*, 2000, 23(1): 19–32.
[12] JIANG Y, HERTEL O, VORMWALD M. An experimental evaluation of three critical plane multiaxial fatigue criteria[J]. *International Journal of Fatigue*, 2007, 29(8): 1 490–1 502.
[13] KALNAUS S, JIANG Y. Fatigue of AL6XN stainless steel[J].

Journal of Engineering Materials and Technology, 2008, 130(3): 1–12.

Biographical notes

WANG Xiaogui, born in 1973, is currently a professor in *College of Mechanical Engineering, Zhejiang University of Technology, China*. His research interests include fatigue fracture, stimulus-responsive hydrogels and interface mechanics.
Tel: +86-571-88320252; E-mail: hpcwxg@zjut.edu.cn

GAO Zengliang, born in 1960, is currently a professor in *College of Mechanical Engineering, Zhejiang University of Technology, China*. His research interests include fatigue fracture and structure integrity.
Tel: +86-571-88320763; E-mail: zlgao@zjut.edu.cn

QIU Baoxiang, born in 1981, was graduated from *Zhejiang University of Technology, China*, in 2009 and is currently a postdoctoral fellow in *Wanxiang Group, Technical Research Center, Hangzhou, China*. His research interests include fatigue fracture and structure integrity of automobiles.
E-mail: origtas@gmail.com

WANG Limei, born in 1984, was graduated from *Zhejiang University of Technology, China*, in 2009, and is currently a PhD candidate in *University of New Mexico, USA*.
E-mail: limei536@163.com

JIANG Yanyao, born in 1963, is professor in *University of Nevada, Reno, USA*. His research interests include cyclic plasticity, elastic-plastic finite element analysis, fatigue and fracture of materials and structures, inelastic constitutive relations, rolling contact analysis, thermo-mechanical behavior, and durability of bolted joints.
Tel: +1-775-7844510; E-mail: yjiang@unr.edu